



## OPEN ACCESS

## EDITED BY

Jinghua Guo,  
Berkeley Lab (DOE), United States

## REVIEWED BY

Xuhui Sun,  
Soochow University, China  
Jyoti Prakash Das,  
Jeju National University, Republic of Korea

## \*CORRESPONDENCE

Seonghyeon Kim,  
✉ shk1014@gnu.ac.kr  
Sanghyun Lee,  
✉ shlee0106@kmu.ac.kr

<sup>†</sup>These authors have contributed equally  
to this work

RECEIVED 17 October 2025

REVISED 21 November 2025

ACCEPTED 09 December 2025

PUBLISHED 05 January 2026

## CITATION

Kang J, Um D-Y, Lee S and Kim S (2026)  
Mechanically stimulated self-powered  
electrochemical sensors: principles,  
classifications, and future directions.  
*Front. Mater.* 12:1727201.  
doi: 10.3389/fmats.2025.1727201

## COPYRIGHT

© 2026 Kang, Um, Lee and Kim. This is an  
open-access article distributed under the  
terms of the [Creative Commons Attribution  
License \(CC BY\)](https://creativecommons.org/licenses/by/4.0/). The use, distribution or  
reproduction in other forums is permitted,  
provided the original author(s) and the  
copyright owner(s) are credited and that the  
original publication in this journal is cited, in  
accordance with accepted academic practice.  
No use, distribution or reproduction is  
permitted which does not comply with  
these terms.

# Mechanically stimulated self-powered electrochemical sensors: principles, classifications, and future directions

Jiseung Kang<sup>1†</sup>, Dae-Yong Um<sup>1†</sup>, Sanghyun Lee<sup>2\*</sup> and Seonghyeon Kim<sup>1\*</sup>

<sup>1</sup>Department of Electrical Engineering, Gyeongsang National University, Jinju, Republic of Korea,

<sup>2</sup>Division of Mechanical Engineering, Korea Maritime and Ocean University, Busan, Republic of Korea

The rapid advancement of self-powered sensor (SPS) technology has enabled continuous and autonomous monitoring across various domains, including biomedical, environmental, and structural applications. Conventional energy-harvesting mechanisms, such as triboelectric, piezoelectric, and electromagnetic induction, produce transient AC-type signals that are prone to drift, attenuation, and poor response under static or low-frequency conditions. Conversely, self-powered electrochemical sensors (SPESs), which operate via mechanically induced modulation of interfacial redox kinetics and ion transport generate stable, quasi-steady-state outputs via Faradaic charge transfer and electrochemical potential variations at the electrode–electrolyte interface. These devices exhibit high sensitivity to both dynamic and static stimuli, presenting operational longevity and material adaptability for long-term sensing applications. Recent advances in hierarchical electrode architectures, multifunctional ionic hydrogels, and hybrid redox systems have further enhanced the energy conversion efficiency, mechanical robustness, and multimodal responsiveness. In this mini-review, we summarize the working mechanisms, material strategies, and classification of mechanically driven SPSs based on the stimulus type. We discuss key challenges such as the limited output power, environmental cross-sensitivity, and reproducibility. Furthermore, we discuss future research directions focused on developing scalable, intelligent, and multimodal self-powered sensing platforms for next-generation IoT and diagnostic systems.

## KEYWORDS

self-powered, electrochemical reaction, sensors, mechanism, redox reaction

## 1 Introduction

The rapid advancement of sensor technology has revolutionized real-time diagnostics and environmental data acquisition across various fields, including biomedical monitoring, health tracking, and wearable electronics (Abdulhussain et al., 2025; Wang et al., 2023; Mamdiwar et al., 2021; Azeem et al., 2025; Tovar-Lopez, 2023). A key area of improvement lies in developing autonomous sensors that are

capable of continuously monitoring physical and physiological conditions over extended periods without depending on bulky or short-lived external power sources (Chatterjee et al., 2023; Conta et al., 2021; Moiş et al., 2018; Dahiya et al., 2020). Self-powered sensors (SPSs), which harvest ambient mechanical or thermal energy and convert it directly into electrical signals, present an effective solution for long-term, maintenance-free operation (Shi and Liu, 2024; Guo et al., 2025; Sohn and Kim, 2021).

Extensive research has been conducted on triboelectric, piezoelectric, and electromagnetic induction-based SPSs owing to their facile design and efficient energy harvesting capabilities (Sreejith et al., 2025; Tang et al., 2023; Rayegani et al., 2022; Han et al., 2023). Recent studies have employed hybrid triboelectric–electrochemical systems for high-efficiency mechanical energy conversion (Das et al., 2024) and additive manufacturing techniques to realize multifunctional electronic and energy-harvesting devices (Divakaran et al., 2022). However, the conventional approaches face limitations in detecting the static pressure, prolonged strain, or low-frequency vibrations—conditions that are frequently encountered in real-world applications (Kim et al., 2020; Wang et al., 2025). Their signals are typically transient and AC-type, and are prone to baseline drift, attenuation, and environmental noise, thereby limiting their suitability for continuous sensing or integration with low-power electronics (Yao et al., 2022; Lu et al., 2021). To overcome these challenges, self-powered electrochemical sensors (SPESs) based on mechanically induced modulation of interfacial redox kinetics and ion transport are a promising alternative (Hasan et al., 2021; Yang et al., 2025; Yang et al., 2024; Gu et al., 2025; Zhang M. et al., 2025; Huang et al., 2024; Zhang X. et al., 2025; Kim et al., 2023).

These devices generate stable and quasi-steady-state signals via Faradaic charge transfer and mechanical perturbation of electrochemical equilibria at the electrode–electrolyte interface (del Campo, 2023; Sailapu and Menon, 2022; Li et al., 2022). Unlike triboelectric and piezoelectric sensors, SPESs exhibit high sensitivity to dynamic inputs as well as static loads and long-term deformations (Lei et al., 2022; Zhang et al., 2022; Jia et al., 2024; Zhang Q. et al., 2023). Their operational versatility and extended signal persistence make them well-suited for applications that require sustained monitoring, such as wearable biosensors, smart environmental systems, and infrastructure integrity diagnostics (Zhang M. et al., 2023; Ren et al., 2023; Saha et al., 2023; Zhang Q. et al., 2023). Recent advances in materials science, such as hierarchical electrode architectures and multifunctional hydrogels, have significantly improved the output stability, mechanical compliance, and signal specificity of SPESs. Furthermore, their functionality has expanded into hybrid domains, such as temperature–mechanical multimodal sensing and real-time wireless integration (Song et al., 2025; Zhang et al., 2024c). Figure 1a depicts the chronological development of self-powered electrochemical sensors (SPESs), from the first galvanic and battery-type configurations to the recent hybrid and multimodal redox-coupled architectures. This evolution demonstrates the transition of self-powered sensing from conventional charge-displacement methods toward stable, mechanically triggered electrochemical mechanisms capable of realizing quasi-steady-state energy conversion. Figure 1b depicts the conceptual framework of this review, outlining the relationship between working mechanisms

(Section 2), classification by stimulus type (Section 3), and potential research implications (Section 4). Thus, these figures present a chronological and structural overview of SPESs.

In this mini-review, we present a comprehensive overview of mechanically stimulated SPESs. We first explain their core working mechanisms and design principles, followed by a classification of the representative devices based on the type of mechanical stimulus: pressure, strain, vibration, and hybrid sensing. Subsequently, we discuss the primary challenges, including the energy output, signal selectivity, mechanical reliability, and performance standardization. Consequently, we propose future research directions that leverage advanced material platforms, algorithmic signal decoupling, and scalable manufacturing techniques. Lastly, we determine the potential for their integration into next-generation autonomous IoT systems and multimodal diagnostic platforms.

## 2 Working mechanism and device architectures of SPESs

SPESs operate via mechanically or environmentally modulated redox reactions triggered by pressure, strain, vibration, temperature, or humidity. These devices typically comprise two electrodes (anode/cathode), an electrolyte medium, and a flexible substrate. Following mechanical deformation, the redox potential difference between the electrodes induces ionic migration and charge transfer through the electrolyte, producing measurable current or voltage outputs (Wu et al., 2020a; Wu et al., 2020b; Wu et al., 2021; Lei et al., 2022; Zhang et al., 2022; Kim et al., 2023; Zhang M. et al., 2023; Huang et al., 2024; Jia et al., 2024; Yang et al., 2024; Zhang H. et al., 2024; Zhang et al., 2024b; Zhang et al., 2024c; Song et al., 2025; Zhang M. et al., 2025; Zhang X. et al., 2025). Unlike conventional sensors powered by external batteries, SPESs utilize spontaneous Faradaic or equilibrium redox reactions, making them inherently autonomous and sustainable.

### 2.1 Basic principles of mechanically triggered electrochemical generation

SPES operation involves converting mechanical energy into electrical energy via mechanically modulated redox coupling. The effective electrode–electrolyte contact area varies under compression or tension, thereby altering the ionic pathways and accelerating the interfacial charge-transfer kinetics (Lei et al., 2022; Kim et al., 2023; Huang et al., 2024; Yang et al., 2024; Zhang M. et al., 2025). For example, an MnO<sub>2</sub>/Carbon–Ag hydrogel system operates over a range of a few Pa to hundreds of kPa and exhibits a sensitivity of  $\approx 14$  mV kPa<sup>-1</sup> with Voc  $\approx 0.927$  V (Yang et al., 2024). Cu/Al galvanic sensors (filter-paper, 2 M LiCl) achieve pressure sensitivities of 0.23 kPa<sup>-1</sup> (1–10 kPa) and 0.01 kPa<sup>-1</sup> (15–30 kPa) (Huang et al., 2024). Mg/Cu systems (LiCl–PVA–CNT) operate over 0.6–100 kPa with sensitivities of 0.738 kPa<sup>-1</sup> (0.6–30 kPa) and 0.166 kPa<sup>-1</sup> (30–100 kPa), and can reach  $\sim 6$  mA/2.75 mW at 100 kPa (Zhang M. et al., 2025). Carbon/Al PDMS-sponge sensors (NaCl/glycerol electrolyte) operate over 0–110 kPa, exhibiting a sensitivity of  $\sim 10$  kPa<sup>-1</sup>

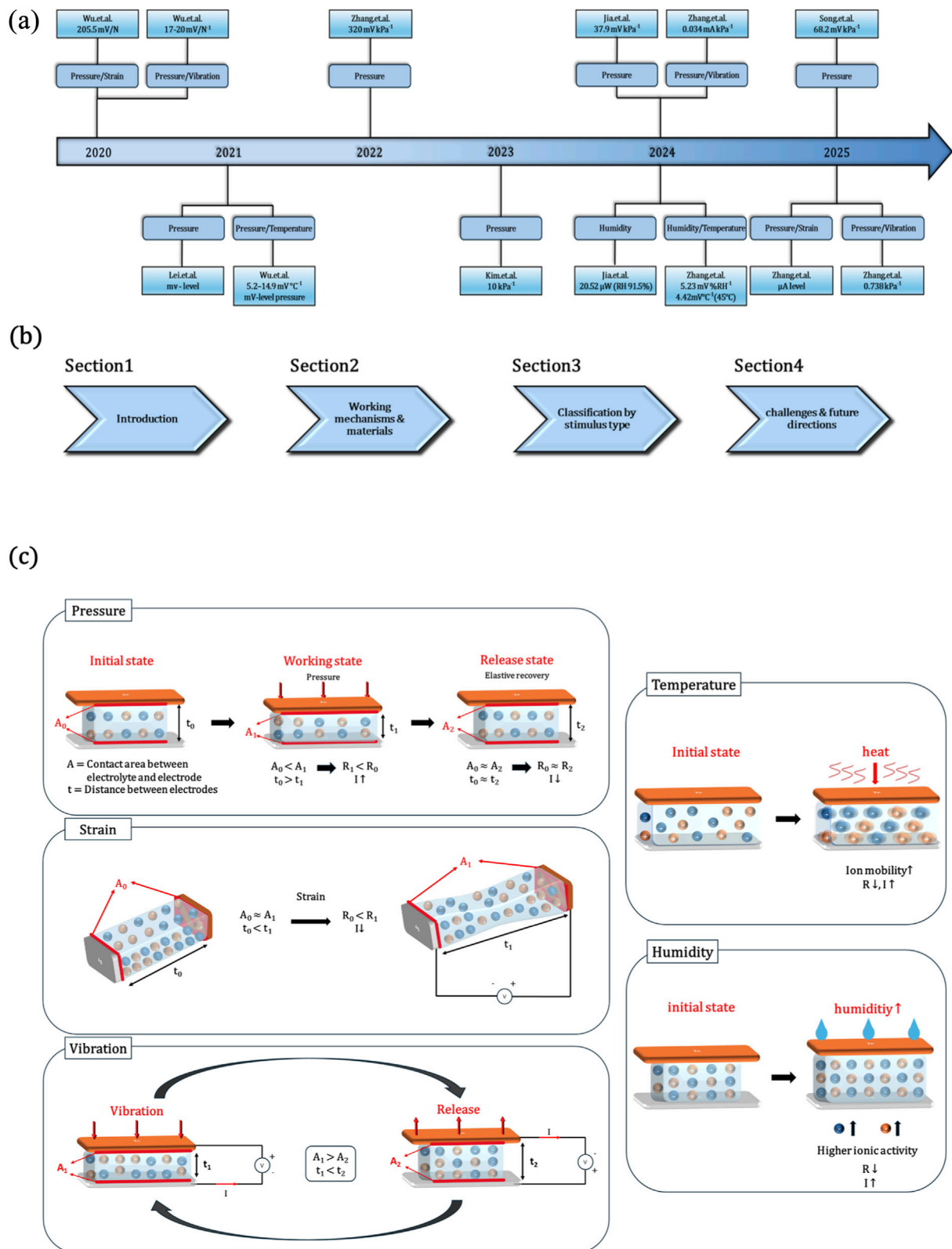


**FIGURE 1** (a) Timeline illustrating the development of self-powered electrochemical sensors (SPESs). (b) Conceptual mind map of the present review. (c) SPESs mechanism (pressure, strain, vibration, humidity, and temperature).

with a rapid response of  $\sim 83$  ms to external pressure stimuli (Kim et al., 2023). rGO/MXene-GO/PVA ionic-channel devices operate over 0.7 Pa–1,300 kPa with mV-level outputs and  $V_{oc} \approx 0.58$  V (Lei et al., 2022). Similarly, potentiometric SPESs, such as Prussian Blue (PB)/AgCl-based e-skins, rely on reversible  $Fe^{2+}/Fe^{3+} \leftrightarrow Ag^0/Ag^+$  equilibria to realize continuous potential variation with high signal stability. The representative PB/Carbon||Ag/AgCl hydrogel sensors exhibit potential sensitivities of  $\sim 205$  mV  $N^{-1}$  (0–1 N) and  $\sim 17$ – $20$  mV  $N^{-1}$  (0.01–10 N), demonstrating reproducible and low-power operation; temperature-coupled designs based on the same redox pair show sensitivities of  $\sim 5.2$ – $14.9$  mV  $^{\circ}C^{-1}$  (Wu et al., 2020a; Wu et al., 2021). Collectively, these Faradaic and equilibrium redox mechanisms enable highly sensitive, low-power mechanical-to-electrical transduction. The working mechanism of SPESs fundamentally varies from that of conventional piezoelectric or triboelectric sensors. SPESs rely on mechanically modulated electrochemical reactions at the electrode–electrolyte interface whereas conventional systems generate transient signals through non-Faradaic charge displacement or contact electrification. Mechanical deformation affects ion transport and redox kinetics, producing quasi-steady-state Faradaic signals that clearly distinguish SPESs from other self-powered sensors.

## 2.2 Redox pairs and application-oriented material choices

Multiple redox couples have been optimized to balance the signal magnitude, durability, and biocompatibility. The Mn/Ag system delivers a high potential difference and long-term stability for repetitive pressure sensing (Yang et al., 2024). The Cu/Al and Mg/Cu galvanic pairs utilize porous paper or CNT-doped polymer frameworks to enhance the ionic mobility and power density (Huang et al., 2024; Zhang M. et al., 2025). A C/Al hydrogel-sponge achieves fast response ( $\sim 83$  ms) and  $\sim 10$  kPa $^{-1}$  sensitivity in the low-pressure regime (Kim et al., 2023). The battery-type Zn/ $VO_2(B)$  and  $MoO_3$ /GO redox pairs form  $Zn^{2+}$ - and  $H^+$ -insertion systems that exhibit long cycle life ( $>10^5$  cycles) and stable pressure–temperature dual sensing (Zhang et al., 2022; Jia et al., 2024). At the equilibrium end, the PB/AgCl and PEDOT:PSS–metal hybrid electrodes present reversible potential shifts owing to sub-nW power consumption (Wu et al., 2020a; Wu et al., 2021). Furthermore, metal–air systems such as Al/ $MnO_2$  utilize moisture-assisted oxygen reduction to deliver OCV  $\approx 1.3$  V and  $\approx 20$   $\mu$ W output for wireless humidity sensing (Zhang M. et al., 2023). Hybrid structures combining Ag or  $MnO_2$  nanoparticles with conductive carbon matrices improve the Faradaic efficiency and mechanical durability (Yang et al., 2024; Zhang M. et al., 2025).

## 2.3 Electrolyte architectures: from biointegration to mechanical stability

The ionic conductivity, stretchability, and environmental endurance are determined based on the electrolytes used. Aqueous NaCl or PBS solutions are biocompatible but are prone to leakage and evaporation. To overcome these

drawbacks, ionic hydrogels such as PVA/LiCl and NaCl/glycerol mixtures present high ionic mobility, flexibility, and anti-drying capability (Wu et al., 2020a; Wu et al., 2021; Kim et al., 2023; Zhang et al., 2024b; Zhang et al., 2024c; Zhang M. et al., 2025). Double-network hydrogels (e.g., PAA/PAM) and ion-gel composites enhance the durability and self-healing ability (Lei et al., 2022; Zhang X. et al., 2025). Solid-state systems using PVDF-HFP-GO or gelatin–chitosan matrices stabilize the Zn-ion and proton-type SPESs, thereby preventing leakage and mechanical fatigue (Zhang et al., 2022; Jia et al., 2024; Song et al., 2025). Hybrid polymer–ionic networks such as PDMS–LiCl and textile-based PVA/NaCl further ensure conformal contact and long-term cyclic operation (Wu et al., 2021; Zhang M. et al., 2023; Zhang et al., 2024b).

## 2.4 Electrode engineering for enhanced signal output

The electrochemical efficiency and mechanical resilience are determined based on the electrode design. Nanostructured graphene, CNT, and porous  $MnO_2$  electrodes enlarge the redox interfaces and accelerate ion exchange (Yang et al., 2024; Zhang M. et al., 2025; Zhang X. et al., 2025). Hybrid structures that combine Ag or  $MnO_2$  nanoparticles with conductive carbon frameworks enhance the Faradaic efficiency and durability (Yang et al., 2024; Zhang M. et al., 2025). Patterned hydrogel electrodes, such as sandpaper-templated or 3D-sponged structures, exhibit uniform stress distribution and stable cycling ( $>10,000$  times) (Kim et al., 2023; Zhang H. et al., 2024). Equilibrium-type PB/AgCl electrodes present stable potential under mechanical strain (Wu et al., 2020a; Wu et al., 2021), whereas prGO and PEDOT:PSS architectures enable anisotropic or multimodal sensing (Wu et al., 2021; Lei et al., 2022). Consequently, optimized electrode morphology enhances the signal-to-noise ratio, mechanical endurance, and multimodal responsiveness in SPESs.

## 2.5 Comparison with triboelectric and piezoelectric sensors

When compared with conventional triboelectric and piezoelectric sensors, SPESs present unique advantages in terms of the signal characteristics and durability. Triboelectric and piezoelectric systems primarily generate AC signals, which are typically susceptible to signal drift, environmental interference, and limited in capturing static stimuli. However, SPESs inherently produce quasi-DC or steady-state outputs. Therefore, they are particularly advantageous for applications that require long-term monitoring under low-frequency or static loading, such as wearable biosensors, structural health monitoring, and passive safety alarms. Furthermore, SPESs are well-suited for more comprehensive sensing scenarios owing to their ability to respond to both dynamic and static mechanical stimuli. Their redox-based mechanisms are less affected by mechanical cycling fatigue, thereby enhancing their reliability for continuous and repeatable measurements.

## 3 Classification of SPESs based on stimulus and applications

SPESs modulate the electrochemical reactions at the electrode–electrolyte interface under mechanical or environmental stimuli. They are broadly classified into the pressure, strain, vibration, temperature, and humidity types (Wu et al., 2020a; Wu et al., 2020b; Wu et al., 2021; Lei et al., 2022; Zhang et al., 2022; Kim et al., 2023; Zhang M. et al., 2023; Huang et al., 2024; Jia et al., 2024; Yang et al., 2024; Zhang H. et al., 2024; Zhang et al., 2024b; Zhang et al., 2024c; Song et al., 2025; Zhang M. et al., 2025; Zhang X. et al., 2025). Each type operates via distinct redox mechanisms and device architectures (Table 1).

In particular, mechanical stimuli can be divided into three major modes that each induce unique electrochemical responses: compressive, tensile, and vibrational. The applied pressure stimuli primarily affect the electrode contact area and interfacial impedance, thereby modulating the Faradaic charge transfer rate and ionic accessibility within the electrolyte. The strain stimuli cause lattice distortion or channel elongation in soft electrolytes, affecting ion pathways and potential distribution under continuous deformation. The vibration stimuli periodically perturb the redox equilibrium, producing quasi-DC outputs synchronized with the mechanical frequency. These distinct deformation modes define the sensing characteristics of SPESs and contribute significantly to tailoring their mechanical and electrochemical coupling behavior.

### 3.1 Pressure-based SPESs

Pressure-sensitive SPESs are the most extensively analyzed owing to their high sensitivity and long-term stability. Devices using Mn/Ag, Cu/Al, Mg/Cu, and C/Al redox pairs exhibit reversible voltage and current under compression (Kim et al., 2023; Huang et al., 2024; Yang et al., 2024; Zhang M. et al., 2025). Hydrogel-sponge architectures with PVA/LiCl or NaCl/glycerol electrolytes achieve sensitivities of up to  $\approx 10 \text{ kPa}^{-1}$  and sub-100 ms response (Kim et al., 2023; Zhang H. et al., 2024). Battery-type Zn/VO<sub>2</sub>(B) and MoO<sub>3</sub>/GO SPESs maintain a stable output of up to  $\sim 500 \text{ kPa}$  (Zhang et al., 2022) and  $524 \text{ kPa}$  (Jia et al., 2024), respectively, with excellent durability. Template-built piezo-electrochemical hybrids (Zhang H. et al., 2024) further enhance the output density and frequency response for both static and dynamic pressure monitoring.

### 3.2 Strain-based SPESs

Strain-responsive SPESs convert tensile deformation into potential or current variation. rGO/MXene potentiometric sensors utilize ion-channel regulation to achieve a stable potential during stretching (Lei et al., 2022). Yarn-type Al/CNT or PEDOT:PSS hybrid architectures maintain the conductivity under  $\approx 200\%$  strain (Wu et al., 2021; Zhang X. et al., 2025), thereby enabling posture tracking, motion detection, and physiological monitoring via continuous potential modulation.

### 3.3 Vibration-based SPESs

Vibration-responsive SPESs exploit periodic deformation to drive coupled piezo-electrochemical processes. Mg/Cu and Zn/Cu hybrid systems generate stable DC outputs during oscillatory cycles (Zhang H. et al., 2024; Zhang M. et al., 2025). PB/AgCl-triboelectric hybrid mechanoreceptors produce dual voltage components, i.e., plateau (static) and spike (dynamic, emulating biological fast and slow-adapting tactile responses (Wu et al., 2020b)). These devices present considerable potential for fatigue monitoring and bioinspired tactile sensing.

### 3.4 Temperature-hybrid SPESs

Multimodal SPESs integrate thermal sensitivity into mechanical transduction by exploiting the temperature dependence of ionic conductivity and redox kinetics. PB/AgCl e-skins present temperature coefficients of  $5.2\text{--}14.9 \text{ mV } ^\circ\text{C}^{-1}$ , thereby supporting wearable health and inflammation monitoring (Wu et al., 2021). Advanced calibration and signal-decoupling schemes ensure reliable operation under dynamic conditions. Humidity-activated SPESs represent an emerging class of environmental self-powered sensors. The Al/MnO<sub>2</sub> metal–air SPES utilizes moisture-assisted oxygen reduction to generate OCV  $\approx 1.32 \text{ V}$  and  $\approx 20 \mu\text{W cm}^{-2}$ , thereby enabling wireless RF humidity monitoring (Zhang M. et al., 2023). Al–C textile micro-galvanic sensors transduce the humidity and temperature variations into potential shifts for respiration analysis (Zhang et al., 2024b). Such devices exhibit autonomous, maintenance-free sensing for environmental, infrastructure, and healthcare applications.

## 4 Challenges and future directions

Mechanically driven SPESs have advanced significantly in terms of their materials, structure, and performance. However, these devices cannot be deployed reliably on a large scale owing to key challenges. These include limited energy output, susceptibility to environmental noise, mechanical instability under repeated deformation, lack of standardized performance metrics, and the requirement for multimodal integration. Addressing these issues is essential for realizing SPES-based platforms for healthcare, environmental monitoring, and autonomous infrastructure diagnostics.

### 4.1 Energy conversion efficiency and output stability

Most SPESs generate low voltage outputs (tens to hundreds of mV) and microampere-level currents, which limit their integration with signal processing and storage components. In particular, electrochemical output becomes unstable under low-frequency or static deformation owing to slow redox kinetics and insufficient ion redistribution. To improve the performance, hierarchical electrode

TABLE 1 Self powered sensor properties.

| Ref. No.     | Stimulus               | Electrode configuration   | Electrolyte/structure  | Sensing range                          | Sensitivity/output   |
|--------------|------------------------|---|--|--|--|
| Yang et al.  | Pressure               | MnO <sub>2</sub> /Carbon    Ag  | PVA-H <sub>3</sub> PO <sub>4</sub> hydrogel (sandpaper template)                 | Pa-hundreds kPa                        | 14 mV kPa <sup>-1</sup> Voc 0.927 V  |
| Zhang et al. | Pressure + strain      | PU/PPy (+)    PU/MXene (-)  | PAA/PAM ion-gel bilayer  | 20 Pa-3.5 MPa                          | Linear current response ( $\mu$ A level)   |
| Huang et al. | Pressure               | Cu    Al  | LiCl (2 M) in filter paper   | 1-30 kPa                               | 0.23 kPa <sup>-1</sup> (1-10 kPa)<br>0.01 kPa <sup>-1</sup> (15-30 kPa)  |
| Zhang et al. | Pressure/vibration     | Mg    Cu  | LiCl + PVA + CNT composite   | 0.6-100 kPa                            | 0.738 kPa <sup>-1</sup> (0.6-30 kPa)<br>0.166 kPa <sup>-1</sup> (30-100 kPa)   |
| Kim et al.   | Pressure               | Carbon    aluminum  | PAAm-coated PDMS sponge + NaCl/Glycerol  | 0-110 kPa                              | 10 kPa <sup>-1</sup> $\Delta$ V 100 mV (83 ms)   |
| Lei et al.   | Pressure               | rGO/MXene   | GO/PVA nanofiber ionic channel   | 0.7 Pa-1,300 kPa                       | mV-level<br>Voc 0.58 V   |
| Zhang et al. | Pressure               | Zn (+)    VO <sub>2</sub> (B)@SS (-)                                  | PVDF-HFP-GO solid electrolyte  | 2 Pa-368 kPa                           | 320 mV kPa <sup>-1</sup> (=2 kPa)<br>4.92 mV kPa <sup>-1</sup> (2-140 kPa)<br>0.57 mV kPa <sup>-1</sup> (140-368 kPa)<br>Voc 0.8 V |
| Jia et al.   | Pressure               | Zn (+)    VO <sub>2</sub> (B)@SS (-)                                  | Gelatin-Chitosan hydrogel + PDMS   | $\leq$ 524 kPa                         | 37.9 mV kPa <sup>-1</sup>  |
| Zhang et al. | Pressure/vibration     | Zn    Cu  | PVA hydrogel w/NH <sub>4</sub> Cl + LiCl   | 0.23-20 kPa                            | 0.034 mA kPa <sup>-1</sup><br>Voc 0.8 V  |
| Zhang et al. | Humidity               | Al (+)    MnO <sub>2</sub> (-)  | NaCl aq. + OH-MWCNT layer  | 10.9%-91.5% RH                         | 20.52 $\mu$ V (RH 91.5%)<br>Voc 1.32 V   |
| Song et al.  | Pressure               | Carbon (top)    Zn (bottom)/V <sub>2</sub> O <sub>5</sub> @C//Zn cell | PVDF-HFP + [EMIM]BF <sub>4</sub> /Zn(BF <sub>4</sub> ) <sub>2</sub> + Nylon mesh | 0-200 kPa                              | 68.2 mV kPa <sup>-1</sup> (0-10 kPa electrolyte 18:8)<br>22.1 mV kPa <sup>-1</sup> (0-30 kPa electrolyte 6:8)                      |
| Zhang et al. | Pressure/touch         | Al    carbon  | Sweat ions (Na <sup>+</sup> /K <sup>+</sup> /Cl <sup>-</sup> ) as electrolyte    | -                                      | 74.6 mv N <sup>-1</sup>  |
| Wu et al.    | Pressure/strain        | PB/Carbon    Ag/AgCl  | PVA/NaCl/Glycerol hydrogel (patterned)   | 0-10 N                                 | 205 mV N <sup>-1</sup> (0-1 N)   |
| Zhang et al. | Humidity + temp        | Al fiber (+)    carbon fiber (-)                                      | PVA/NaCl/Glycerol textile gel  | -                                      | 5.23 mV %RH <sup>-1</sup> (RH 97%)<br>4.42 mV $^{\circ}$ C <sup>-1</sup> (45 $^{\circ}$ C)   |
| Wu et al.    | Pressure/vibration     | PB/Carbon    Ag/AgCl  | PVA/NaCl/Glycerol hydrogel (micro-patterned)                                     | 0.01-10 N                              | 17-20 mV N <sup>-1</sup>   |
| Wu et al.    | Temperature + pressure | PB/Carbon    Ag/AgCl  | PVA/NaCl/Glycerol hydrogel (glycerol-ratio tuned)                                | 5 $^{\circ}$ C-50 $^{\circ}$ C kPa-MPa | 5.2-14.9 mV $^{\circ}$ C <sup>-1</sup> /mV-level pressure  |

structures using hybrids or porous foams have been developed to enhance the ionic mobility and active surface area, thereby achieving higher power density. Metallic electrodes present better conductivity but are rigid, whereas carbon-based materials are flexible but yield lower output. Hybrid composites that integrate carbon nanotubes, conducting polymers (e.g., PEDOT:PSS), and Ag nanoparticles present considerable potential for balancing the flexibility and performance.

## 4.2 Signal selectivity and environmental noise

SPESs operate based on the interfacial redox reactions, making them sensitive to external factors such as temperature, humidity, and pH. This noise sensitivity is a major challenge in wearable and biomedical contexts, where body fluids (e.g., sweat) or ambient humidity can distort the ionic conductivity and electrode

potential. Surface modification with ion-selective membranes or ion-imprinted polymers has improved the selectivity by enabling specific ion detection under mechanical modulation. Additionally, real-time signal denoising using lightweight machine learning algorithms yielded a classification accuracy of over 95%, even with noisy input signals. However, integrating such signal processing within ultra-low-power hardware remains a major challenge for autonomous applications.

### 4.3 Mechanical durability and long-term reliability

Hydrogel-based electrolytes present excellent flexibility and biocompatibility; however, they are susceptible to dehydration, mechanical rupture, and fatigue. Electrode delamination and microcrack propagation under cyclic deformation (>10,000 cycles) cause long-term performance degradation. Double-network or toughened ionic hydrogels have been developed to overcome this challenge by providing enhanced mechanical stability and water retention. Furthermore, encapsulation techniques using elastomeric coatings and self-healing interlayers present considerable potential in improving device lifetime under real-use scenarios.

### 4.4 Standardization and reproducibility

The lack of standardized testing and reporting protocols limits the reproducibility and industrial scalability. Variations in the electrolyte type, electrode architecture, and loading conditions make it difficult to compare studies across different research groups. Ongoing efforts aim to establish standardized performance metrics such as areal sensitivity ( $V/kPa \cdot cm^2$ ), response stability under  $N$  cycles, and normalized power density ( $\mu W/cm^2$ ). Furthermore, we proposed the integration of plug-and-play device modules with wireless connectivity for benchmarking under field conditions.

### 4.5 Future perspectives

Future SPES systems are expected to evolve into intelligent and multimodal platforms that can simultaneously detect mechanical, thermal, and even chemical cues. For instance, fiber-based architectures that integrate ionic gels with temperature-responsive elements demonstrate dual-mode sensing of strain and temperature. However, advanced calibration algorithms and embedded low-power computing are required for accurate signal decoupling and mitigation of cross-sensitivity. Emerging materials, including MOFs for enhanced ionic transport, anti-drying ion gels for long-term operational stability, and soft interpenetrating networks for mechanical resilience, can advance both the robustness and ionic conductivity in next-generation SPESs. Furthermore, scalable

fabrication approaches, such as inkjet printing, laser patterning, and roll-to-roll processing are crucial for large-area, cost-effective integration of SPES arrays into smart wearables, soft robotics, and infrastructure monitoring systems.

## Author contributions

JK: Conceptualization, Writing – original draft, Writing – review and editing, Methodology. D-YU: Investigation, Writing – original draft, Writing – review and editing, Visualization. SL: Supervision, Writing – original draft, Writing – review and editing, Methodology. SK: Funding acquisition, Supervision, Writing – original draft, Writing – review and editing.

## Funding

The author(s) declared that financial support was received for this work and/or its publication. This work was supported by the National Research Foundation of Korea (NRF) grant funded by the Korean government (MSIT) (RS-2025-00518047); and the Glocal University 30 Project Fund of Gyeongsang National University in 2025.

## Conflict of interest

The author(s) declared that this work was conducted in the absence of any commercial or financial relationships that could be construed as a potential conflict of interest.

## Generative AI statement

The author(s) declared that generative AI was not used in the creation of this manuscript.

Any alternative text (alt text) provided alongside figures in this article has been generated by Frontiers with the support of artificial intelligence and reasonable efforts have been made to ensure accuracy, including review by the authors wherever possible. If you identify any issues, please contact us.

## Publisher's note

All claims expressed in this article are solely those of the authors and do not necessarily represent those of their affiliated organizations, or those of the publisher, the editors and the reviewers. Any product that may be evaluated in this article, or claim that may be made by its manufacturer, is not guaranteed or endorsed by the publisher.

## References

Abdulhussain, S. H., Mahmmud, B. M., Alwhelat, A., Shehada, D., Shihab, Z. I., Mohammed, H. J., et al. (2025). A comprehensive review of sensor technologies

in IoT: technical aspects, challenges, and future directions. *Computers* 14, 342. doi:10.3390/computers14080342

- Azeem, M., Shahid, M., Masin, I., and Petru, M. (2025). Design and development of textile-based wearable sensors for real-time biomedical monitoring: a review. *J. Text. Inst.* 116, 80–95. doi:10.1080/00405000.2024.2318500
- Chatterjee, B., Mohseni, P., and Sen, S. (2023). Bioelectronic sensor nodes for the internet of bodies. *Annu. Rev. Biomed. Eng.* 25, 101–129. doi:10.1146/annurev-bioeng-110220-112448
- Conta, G., Libanori, A., Tat, T., Chen, G., and Chen, J. (2021). Triboelectric nanogenerators for therapeutic electrical stimulation. *Adv. Mater.* 33, e2007502. doi:10.1002/adma.202007502
- Dahiya, A. S., Thireau, J., Boudaden, J., Lal, S., Gulzar, U., Zhang, Y., et al. (2020). Review—energy autonomous wearable sensors for smart healthcare: a review. *J. Electrochem. Soc.* 167, 037516. doi:10.1149/2.0162003JES
- Das, J. P., Nardekar, S. S., Ravichandran, V., and Kim, S. J. (2024). From friction to function: a high-voltage sliding triboelectric nanogenerator for highly efficient energy autonomous IoTs and self-powered actuation. *Small* 20 (48), 2405792. doi:10.1002/sml.202405792
- del Campo, F. J. (2023). Self-powered electrochemical sensors. *Curr. Opin. Electrochem.* 41, 101356. doi:10.1016/j.coelec.2023.101356
- Divakaran, N., Das, J. P., Pv, A. K., Mohanty, S., Ramadoss, A., and Nayak, S. K. (2022). Comprehensive review on various additive manufacturing techniques and its implementation in electronic devices. *J. Manuf. Syst.* 62, 477–502. doi:10.1016/j.jmsy.2022.01.002
- Gu, Y., Luo, Y., Guo, Q., Yu, W., Li, P., Wang, X., et al. (2025). Empowering human-machine interfaces: self-powered hydrogel sensors for flexible and intelligent systems. *Adv. Funct. Mater.* e09085. doi:10.1002/adfm.202509085
- Guo, S., Patel, S., Wang, J., Yu, Z., Qu, H., Zhang, S., et al. (2025). Self-powered green energy-harvesting and sensing interfaces based on hydroscopic gel and water-locking effects. *Sci. Adv.* 11, eadw5991. doi:10.1126/sciadv.adw5991
- Han, Y., He, L., Sun, L., Wang, H., Zhang, Z., and Cheng, G. (2023). A review of piezoelectric-electromagnetic hybrid energy harvesters for different applications. *Rev. Sci. Instrum.* 94, 101501. doi:10.1063/5.0161822
- Hasan, M. A. M., Wu, H., and Yang, Y. (2021). Redox-induced electricity for energy scavenging and self-powered sensors. *J. Mater. Chem. A* 9, 19116–19148. doi:10.1039/D1TA02287C
- Huang, Z., Duan, Z., Huang, Q., Yuan, Z., Jiang, Y., and Tai, H. (2024). A facile fabricated electrochemical self-powered pressure sensor for multifunctional applications. *J. Mater. Chem. C* 12, 18320–18326. doi:10.1039/d4tc03434a
- Jia, P., Zhang, Q., Ren, Z., Yin, J., Lei, D., Lu, W., et al. (2024). Self-powered flexible battery pressure sensor based on gelatin. *Chem. Eng. J.* 479, 147586. doi:10.1016/j.cej.2023.147586
- Kim, D. W., Lee, J. H., Kim, J. K., and Jeong, U. (2020). Material aspects of triboelectric energy generation and sensors. *NPG Asia Mater* 12, 6. doi:10.1038/s41427-019-0176-0
- Kim, S., Cho, W., Hwang, J., and Kim, J. (2023). Self-powered pressure sensor for detecting static and dynamic stimuli through electrochemical reactions. *Nano Energy* 107, 108109. doi:10.1016/j.nanoen.2022.108109
- Lei, D., Zhang, Q., Liu, N., Su, T., Wang, L., Ren, Z., et al. (2022). An ion channel-induced self-powered flexible pressure sensor based on potentiometric transduction mechanism. *Adv. Funct. Mater.* 32, 2108856. doi:10.1002/adfm.2021108856
- Li, S., Zhang, Y., Liang, X., Wang, H., Lu, H., Zhu, M., et al. (2022). Humidity-sensitive chemoelectric flexible sensors based on metal-air redox reaction for health management. *Nat. Commun.* 13, 5416. doi:10.1038/s41467-022-33133-y
- Lu, S., Lei, W., Gao, L., Chen, X., Tong, D., Yuan, P., et al. (2021). Regulating the high voltage and high-impedance characteristics of triboelectric nanogenerator toward practical self-powered sensors. *Nano Energy* 87, 106137. doi:10.1016/j.nanoen.2021.106137
- Mamdiwar, S. D., R, A., Shakruwala, Z., Chadha, U., Srinivasan, K., and Chang, C. Y. (2021). Recent advances on IoT-assisted wearable sensor systems for healthcare monitoring. *Biosensors* 11, 372. doi:10.3390/bios11100372
- Moïş, G. D., Sanislav, T., Folea, S. C., and Zeadally, S. (2018). Performance evaluation of energy-autonomous sensors using power-harvesting beacons for environmental monitoring in internet of things (IoT). *Sensors (Basel)* 18, 1709. doi:10.3390/s18061709
- Rayegani, A., Saberian, M., Delshad, Z., Liang, J., Sadiq, M., Nazar, A. M., et al. (2022). Recent advances in self-powered wearable sensors based on piezoelectric and triboelectric nanogenerators. *Biosensors* 13, 37. doi:10.3390/bios13010037
- Ren, Z., Zhang, H., Liu, N., Lei, D., Zhang, Q., Su, T., et al. (2023). Self-powered 2D nanofluidic graphene pressure sensor with serosa-mimetic structure. *EcoMat* 5, e12299. doi:10.1002/eom.2.12299
- Saha, K., Chatterjee, A., Das, A., Ghorai, A., and Jeong, U. (2023). Self-powered ionic tactile sensors. *J. Mater. Chem. C* 11, 7920–7936. doi:10.1039/d2tc05109e
- Sailapu, S. K., and Menon, C. (2022). Engineering self-powered electrochemical sensors using analyzed liquid sample as the sole energy source. *Adv. Sci. (Weinh)* 9, e2203690. doi:10.1002/advs.202203690
- Shi, Q., and Liu, H. (2024). Energy harvesters and self-powered sensors for smart electronics, 2nd edition. *Micromachines* 15, 99. doi:10.3390/mi15010099
- Sohn, K. R., and Kim, H. S. (2021). A magnetic energy harvesting device using current transformer. *J. Adv.* 45, 307–311. doi:10.5916/jam.2021.45.5.307
- Song, Y., Zhang, Y., Lin, S., Long, Z., Chen, S., Tan, H., et al. (2025). Synergistic fusion of mechanotransduction and power supplying functions towards highly compact and fully self-powered smart wearables. *Nano Energy* 134, 110524. doi:10.1016/j.nanoen.2024.110524
- Sreejith, S., Ajayan, J., Reddy, N. V. U., Mathew, J. K., and Manikandan, M. (2025). Advances in self-powered sensing with triboelectric nanogenerators: a review. *Sens. Imaging* 26, 73. doi:10.1007/s11220-025-00596-4
- Tang, W., Sun, Q., and Wang, Z. L. (2023). Self-powered sensing in wearable electronics—a paradigm shift technology. *Chem. Rev.* 123, 12105–12134. doi:10.1021/acs.chemrev.3c00305
- Tovar-Lopez, F. J. (2023). Recent progress in micro- and nanotechnology-enabled sensors for biomedical and environmental challenges. *Sensors (Basel)* 23, 5406. doi:10.3390/s23125406
- Wang, C., He, T., Zhou, H., Zhang, Z., and Lee, C. (2023). Artificial intelligence enhanced sensors-enabling technologies to next-generation healthcare and biomedical platform. *Bioelectron. Med.* 9, 17. doi:10.1186/s42234-023-00118-1
- Wang, Y., Mu, H., He, S., Wang, S., Shen, M., and Zhang, G. (2025). High-performance energy harvesting device and self-powered wide-range pressure sensor with microstructure and porous synergy. *Chem. Eng. J.* 516, 164139. doi:10.1016/j.cej.2025.164139
- Wu, X., Ahmed, M., Khan, Y., Payne, M. E., Zhu, J., Lu, C., et al. (2020a). A potentiometric mechanotransduction mechanism for novel electronic skins. *Sci. Adv.* 6, eaba1062. doi:10.1126/sciadv.aba1062
- Wu, X., Zhu, J., Evans, J. W., and Arias, A. C. (2020b). A single-mode, self-adapting, and self-powered mechanoreceptor based on a potentiometric-triboelectric hybridized sensing mechanism for resolving complex stimuli. *Adv. Mater.* 32, e2005970. doi:10.1002/adma.202005970
- Wu, X., Zhu, J., Evans, J. W., Lu, C., and Arias, A. C. (2021). A potentiometric electronic skin for thermosensation and mechanosensation. *Adv. Funct. Mater.* 31, 2010824. doi:10.1002/adfm.202010824
- Yang, Z., Wang, Q., Yu, H., Xu, Q., Li, Y., Cao, M., et al. (2024). Self-powered biomimetic pressure sensor based on Mn–Ag electrochemical reaction for monitoring rehabilitation training of athletes. *Adv. Sci. (Weinh)* 11, e2401515. doi:10.1002/advs.202401515
- Yang, B., Wang, L., and Sun, B. (2025). Advances in self-powered electrochemical systems for sports applications: harnessing energy and sensing. *Int. J. Electrochem. Sci.* 20, 101080. doi:10.1016/j.ijoes.2025.101080
- Yao, L., Zhang, H., Jiang, J., Zhang, Z., and Zheng, X. (2022). Recent progress in sensing technology based on triboelectric nanogenerators in dynamic behaviors. *Sensors (Basel)* 22, 4837. doi:10.3390/s22134837
- Zhang, Q., Lei, D., Liu, N., Liu, Z., Ren, Z., Yin, J., et al. (2022). A zinc-ion battery-type self-powered pressure sensor with long service life. *Adv. Mater.* 34, e2205369. doi:10.1002/adma.202205369
- Zhang, M., Duan, Z., Zhang, B., Yuan, Z., Zhao, Q., Jiang, Y., et al. (2023a). Electrochemical humidity sensor enabled self-powered wireless humidity detection system. *Nano Energy* 115, 108745. doi:10.1016/j.nanoen.2023.108745
- Zhang, Q., Lei, D., Shi, J., Ren, Z., Yin, J., Jia, P., et al. (2023b). Pressure-regulated nanoconfined channels for highly effective mechanical-electrical conversion in proton battery-type self-powered pressure sensor. *Adv. Mater.* 35, e2308795. doi:10.1002/adma.202308795
- Zhang, H., Fang, Y., Lee, J., Jeong, C. K., and Zhang, Y. (2024a). Templates-built structural designs for piezoelectrochemical pressure sensors. *ACS Appl. Mater. Interfaces.* 16, 62617–62626. doi:10.1021/acsami.4c12507
- Zhang, J., Ren, W., Chen, S., Wang, R., Luo, H., Diao, Y., et al. (2024b). Facile construction of self-powered electronic textiles for comprehensive respiration analysis. *Adv. Intell. Syst.* 6, 2300558. doi:10.1002/aisy.202300558
- Zhang, J., Zhang, H., Ren, W., Gong, W., Lu, Y., Li, Y., et al. (2024c). Skin-triggered electrochemical touch sensation for self-powered human-machine interfacing. *Sens. Actuators B* 406, 135443. doi:10.1016/j.snb.2024.135443
- Zhang, M., Duan, Z., Huang, Z., Yu, H., Wang, C., Zhang, H., et al. (2025a). Constructing a high-power self-powered electrochemical pressure sensor for multimode pressure detections. *Nano Energy* 136, 110747. doi:10.1016/j.nanoen.2025.110747
- Zhang, X., Wang, S., Liang, X., Liu, M., Zhang, Z., and Zu, G. (2025b). Highly stretchable supercapacitor-type multifunctional self-powered porous electronic skins. *Adv. Funct. Mater.* 35, 2415640. doi:10.1002/adfm.202415640